Metaphase to Anaphase (*mat*) Transition–defective Mutants in *Caenorhabditis elegans*

Andy Golden,* Penny L. Sadler,‡§ Matthew R. Wallenfang,‖ Jill M. Schumacher,¶ Danielle R. Hamill, Gayle Bates,§ Bruce Bowerman,** Geraldine Seydoux,‖ and Diane C. Shakes§**

*Laboratory of Biochemistry and Genetics, National Institute of Diabetes and Digestive and Kidney Diseases, National Institutes of Health, Bethesda, Maryland 20892; ‡Department of Biology, University of Houston, Houston, Texas 77204; §Department of Biology, College of William and Mary, Williamsburg, Virginia 23187; ‖Department of Molecular Biology and Genetics, Johns Hopkins University School of Medicine, Baltimore, Maryland 21205; ¶Department of Molecular Genetics, University of Texas, M.D. Anderson Cancer Center, Houston, Texas 77030; and **Institute of Molecular Biology, University of Oregon, Eugene, Oregon 97403

Abstract. The metaphase to anaphase transition is a critical stage of the eukaryotic cell cycle, and, thus, it is highly regulated. Errors during this transition can lead to chromosome segregation defects and death of the organism. In genetic screens for temperature-sensitive maternal effect embryonic lethal (Mel) mutants, we have identified 32 mutants in the nematode *Caenorhabditis elegans* in which fertilized embryos arrest as one-cell embryos. In these mutant embryos, the oocyte chromosomes arrest in metaphase of meiosis I without transitioning to anaphase or producing polar bodies. An additional block in M phase exit is evidenced by the failure to form pronuclei and the persistence of phosphohistone H3 and MPM-2 antibody staining. Spermatocyte meiosis is also perturbed; primary spermatocytes arrest in metaphase of meiosis I and fail to produce secondary spermatocytes. Analogous mitotic defects cause M phase delays in mitotic germline proliferation. We have named this class of mutants "*mat*" for metaphase to anaphase transition defective. These mutants, representing six different complementation groups, all map near genes that encode subunits of the anaphase promoting complex or cyclosome, and, here, we show that one of the genes, *emb-27*, encodes the *C. elegans* CDC16 ortholog.

Key words: meiosis • metaphase arrest • cell cycle • *C. elegans* • anaphase promoting complex

Introduction

Eukaryotic cell division is a highly regulated process during which cells duplicate their chromosomes, align them at a metaphase plate, and then segregate them equally to each of their two daughter cells. Accurate chromosome segregation during the metaphase to anaphase transition is essential for proper cell function, since errors in chromosome segregation can lead to cell death, sterility, birth defects, or malignant cancers. Not surprisingly, genetic studies of yeast mitosis suggest that the transition out of metaphase and through anaphase is highly regulated both in terms of the sequence of events and the existence of checkpoint regulators. Driving the process forward is a multiprotein E3–ubiquitin ligase complex known as the anaphase promoting complex or cyclosome (APC/C)[1] that functions to sequentially target key cellular components for proteolytic destruction (Zachariae and Nasmyth, 1999). APC/C initiates the metaphase to anaphase transition by first targeting the destruction of the anaphase inhibitor Pds1/Cut2 (Yamamoto et al., 1996) whose absence permits the separation of sister chromatids (Ciosk et al., 1998). APC/C then drives the process forward as it subsequently targets Ase1 and cyclin B for destruction (Peters, 1999). Ase1 destruction permits spindle elongation during anaphase B (Juang et al., 1997), and cyclin B destruction permits M phase exit.

Cells must avoid premature activation of APC/C and precocious exit from metaphase, because once chromosomes separate during anaphase, defects stemming from misaligned or stray chromosomes can no longer be corrected. The idea that cells might have a metaphase checkpoint (also called spindle assembly checkpoint or kinetochore attachment checkpoint) was first suggested by the observation that cells treated with microtubule inhibitors arrest in a metaphase-like state (Eigsti and Dustin, 1957). Recently, this arrest has been shown to be mediated by a set of checkpoint proteins that specifically block the activity of the APC/C in the presence of either abnormal spindles or unattached kinetochores (for review see Gardner and Burke, 2000).

A. Golden and P.L. Sadler contributed equally to this work.

Address correspondence to Diane Shakes, Department of Biology, College of William and Mary, P.O. Box 8795, Williamsburg, VA 23187. Tel.: (757) 221-2409. Fax: (757) 221-6483. E-mail: dcshak@wm.edu

[1]*Abbreviations used in this paper:* APC/C, anaphase promoting complex or cyclosome; CDK, cyclin-dependent kinase; DAPI, 4,6-diamidino-2-phenylindole; DIC, differential interference contrast; Mel, maternal effect embryonic lethal; RNAi, RNA-mediated interference; Ste, sterile; TPR, tetratricopeptide repeat; ts, temperature sensitive.

A combination of genetic, cytological, and biochemical studies has elucidated many of the molecular mechanisms that underlie these critical cell cycle controls (Murray and Hunt, 1993; Nasmyth et al., 2000). These studies reveal that the same basic mechanisms drive the processes of cell division and chromosome separation in both yeast and animal cells, and that many key players are highly conserved in their molecular sequences. Nevertheless, given that many cells differ in the specific details of their cell division processes, underlying mechanistic differences are also likely to exist. For instance, animal cells disassemble their nuclear envelopes before chromosome separation, but yeasts do not. Since the mitotic proteins of yeasts and animal cells function within distinctive cellular environments, they may also be regulated differently. Likewise, the mechanisms that separate sister chromatids during mitosis and meiosis II may differ from those that separate chiasmatically linked homologous chromosomes during meiosis I. Although the loss of sister chromatid cohesion is critical for all of these divisions, centromeric cohesion is specifically protected only during meiosis I (Miyazaki and Orr-Weaver, 1994; van Heemst and Heyting, 2000). On the other hand, both the APC/C target, Pds1, and the APC/C regulator, MAD2, have been recently shown to regulate the separation of not only sister chromatids, but also homologous chromosomes (Salah and Nasmyth, 2000; Shonn et al., 2000). Another largely unexplored area of investigation is whether APC/C-related proteins and their substrates function differently during oocyte and spermatocyte meiosis, given that oocyte meiosis occurs on an acentriolar spindle, whereas sperm meiosis employs a centriole-based spindle.

Here, we present the isolation and analysis of a collection of temperature-sensitive (ts) mutants in the nematode *Caenorhabditis elegans* whose defects specifically block the metaphase to anaphase transition during the germline mitotic and meiotic divisions. Furthermore, we show that at least one of these genes encodes a subunit of the APC/C. This mutant collection provides an important addition to the analysis of the metaphase to anaphase transition for several reasons. First, because the alleles are ts, they can be used to analyze the role of essential genes during gametogenesis. Such analysis would not be possible in null mutants of genes that are required for the early mitotic divisions of either the soma or the developing germline. Second, because the germline is the only tissue in *C. elegans* adults that continues to undergo cell divisions, adult upshift experiments allow germline-specific defects to be studied in the absence of complicating somatic defects. Third, these germline cell divisions are both interesting and distinct for the following reasons. (a) A unique aspect of meiosis I is that the paired homologues are linked by chiasmata. (b) Oocyte and spermatocyte meiosis differ drastically in their associated spindle structures and cytokinesis patterns. (c) Mitotically dividing germ cell nuclei exhibit an intriguing cell cycle independence despite the fact that they are cytoplasmically linked (Hirsh et al., 1976). (d) Finally, because the meiotic germ cells are arranged in temporal order along the distal–proximal axis of the adult gonad, sequential stages of meiosis can be easily observed. With a focus on the metaphase to anaphase transition, this collection of ts mutants provides a unique opportunity to compare the phenotypic consequences of M phase defects during three different types of cell divisions: oocyte meiosis, spermatocyte meiosis, and germline mitosis.

Materials and Methods

Genetic Screen for Ts Embryonic Lethal Mutants

Ts embryonic lethal mutants were isolated in two separate genetic screens, both modified from Kemphues et al. (1988). All steps were carried out at 15°C, except where noted. The *ax* alleles were isolated as follows: L4 hermaphrodites of the genotype *him-3 (e1147) IV*; *lin-2 (e1309) axIs36 X* were mutagenized with 25 mM ethyl methanesulfonate using standard procedures (Brenner, 1974). *lin-2* mutant hermaphrodites lack a functional vulva, and, thus, retain most of their progeny in their uteri. *axIs36* is a chromosomally integrated transgene containing a *pes-10:GFP* fusion that was used in a secondary screen not described here (Wallenfang, M. and G. Seydoux, unpublished results). F2 animals, synchronized by hypochlorite treatment of F1 gravid adults (Emmons et al., 1979), were shifted as L4 larvae to 25°C for 20 h and back down to 15°C for an additional 20 h. F2 adults containing dead embryos were transferred individually to new plates at 15°C. 3 d later, plates were examined for the presence of viable F3 progeny, indicating an embryonic lethal mutant was rescued by the shift to the permissive temperature. From ~900,000 mutagenized genomes, 1,197 ts embryonic lethal mutants were isolated. With the protocol used, most, but perhaps not all, of these alleles are independent. The terminal phenotypes of these mutants was determined in a secondary screen by shifting L4 hermaphrodites to 25°C for 12–16 h and viewing the accumulated in utero embryos under DIC (differential interference contrast) optics on a Zeiss Axioplan II compound microscope (ZEISS). From 1,197 ts embryonic lethal mutants, we recovered 30 mutants that arrest at the one-cell stage. Five of these one-cell arrested mutants have cytokinesis defects and will not be described here. The remaining 25 *ax* alleles are the subject of this report.

The *or* alleles described here were isolated in a similar screen, except for the following differences: the starting *lin-2* strain lacked *him* mutations and integrated transgenes, ethyl methanesulfonate was used at 20 mM, and F2 animals were upshifted as L4 larvae for 25–30 h. For screening, F2 animals were suspended in M9 buffer, and bloated animals containing dead embryos were transferred individually to new plates at 15°C. From ~1,000,000 mutagenized genomes, ~300 ts embryonic lethal mutants were isolated. Of these, 14 mutants arrested at the one-cell stage. Seven of these are described here, and the remaining seven have unrelated cytokinesis defects (Encalada et al., 2000).

Strains and Alleles

The Bristol strain N2 was used as the standard wild-type strain. The marker mutations, deficiencies, and balancer chromosomes used are listed by chromosome as follows: LGI: *dpy-5(e61)*, *unc-13(e450)*, *bli-4(e937)*, *dpy-14(e188)*, *unc-74(x19)*, *unc-38(x20)*, *unc-63(x18)*, *hDf6*, *sDf4*, *hDp31(I;f)*; LGII: *rol-1(e91), unc-4(e120), bli-1(e769), unc-53(e404)*, *mnDf90*, *mnDf86*, *mnDf77*, *mnC1 (dpy-10[e128] unc-52[e444])*; LGIII: *unc-32(e189)*, *dpy-19(e1259)*, *glp-1(q339)*, *daf-7(e1372ts)*, *dpy-1(e1)*, *unc-36(e251)*, *tDf9*, *mnDp37 (III;f)*; LGIV: *him-3(e1147)*, *him-8(e1489)*; LGV: *him-5(e1490)*; and LGX: *lin-2(e1309)*. Culturing, handling, and genetic manipulations of *C. elegans* were performed using standard procedures (Brenner, 1974).

Genetic Analysis

Newly isolated mutations were outcrossed three to five times, and complementation was tested to one another until map positions were established. Linkage analysis, deficiency complementation, two factor mapping, and three factor mapping were used to map the three *mat* loci and the new alleles of *emb-27* and *emb-30*. Additional *emb-27* and *emb-30* map data was reported previously (Cassada et al., 1981; Sigurdson et al., 1984; Furuta et al., 2000). Our mapping crosses place *mat-1* on LGI close to, or left of, *unc-63*. Deficiency crosses place *mat-2* on LGII between the left breakpoint of *mnDf87* and the right breakpoint of *mnDf90*, but not under either *mnDf86* or *mnDf87*. *mat-3* maps left of *dpy-1* and *daf-7* on the far left arm of LGIII (see Fig. 2). Data from these crosses are available from the *C. elegans* database WormBase (http://www.wormbase.org). Because *mat-1*(*ax72)* and *mat-1*(*ax520)* homozygotes were difficult to maintain at 15°C,

these alleles were maintained as heterozygotes over an *unc-38(x20) dpy-5(e61)* chromosome. Likewise, *emb-27*(*ax189*) was maintained over the *mnC1* balancer chromosome. Because *mat-1(ax212*) is leaky at 25°C, it was characterized at 26°C. To facilitate complementation tests and the analysis of male phenotypes, genetic doubles of various *mat* alleles with either *him-5(V)* or *him-8(IV)* were constructed; all male and spermatogenesis phenotypes were secondarily confirmed in *him/+* strains.

Growth Conditions

Mutant stocks were maintained at either 15 or 16°C. For the two-cell embryo shift-up experiments, adult hermaphrodites were raised at 15°C, and then dissected in a drop of egg salts (Edgar, 1995), using 27.5 gauge needles. Isolated two-cell embryos were transferred to prewarmed 25.5°C plates for further development. In L1 upshift experiments, threefold embryos were picked to fresh plates at 15°C and shifted to 25.5°C after hatching. Alternatively, L1s were directly picked from 15 to 25.5°C. For the analysis of spermatocyte meiosis defects, *him-8* doubles of *mat* mutants were grown at 16°C until the late L3 larval stage. Males were then picked to fresh plates and grown at 25.5°C until they reached early adulthood. For the analysis of embryos and gonads within somatically unaffected adults, young adult hermaphrodites with few, if any, embryos in their uteri were upshifted to 25.5°C for 6–7 h. Embryos and gonads were then isolated for analysis, as described below. For many alleles, it proved essential to maintain the incubators at 25.5 ± 0.5°C to attain fully penetrate mutant phenotypes.

Immunohistochemistry and Other Phenotypic Analysis

For the analysis of early embryos and hermaphrodite gonads, upshifted adult hermaphrodites were transferred to a 5-μl drop of egg buffer (Edgar, 1995) on a slide subbed with poly-L-lysine (Sigma-Aldrich). Embryos and gonads were released using 27.5 gauge needles, freeze–cracked, and processed for antibody staining (Miller and Shakes, 1995). For tubulin immunostaining, embryos were fixed in −20°C methanol for at least 1 h. After three washes in PBS, the slides were blocked for 1 h in PBS containing 0.5% BSA and 0.1% Tween 20 before a 2 h room temperature incubation with 1:100 FITC-conjugated anti–α-tubulin antibodies (DM1A; Sigma-Aldrich) (Blose et al., 1984). 4,6-diamidino-2-phenylindole (DAPI) (1 μg/ml) was added during the last 5 min. After a brief wash in PBS, the slides were mounted using either Anti-Fade (Molecular Probes) or Gel/Mount (Biomeda Corp.). Other immunostaining protocols were similar. Specimens were incubated at room temperature with 1:100 anti-phosphohistone H3 polyclonal antibody (Upstate Biotechnology) (Hendzel et al., 1997) for 3 h and rhodamine-conjugated anti–rabbit secondary IgG (Sigma-Aldrich) for 2 h. Specimens were incubated with 1:500 MPM-2 monoclonal antibody (Dako) (Davis et al., 1983) for 16–20 h at 4°C and with rhodamine-conjugated anti–mouse IgG (Jackson ImmunoResearch Laboratories) for 2 h at room temperature. In some cases, DAPI was added directly to the mounting media.

Meiotic sperm spreads were generated for Hoechst/DIC analysis by dissecting male gonads in egg buffer (Edgar, 1995) containing 100 μg/ml of lipid soluble DNA-binding Hoechst dye 33342 (Sigma-Aldrich). A coverslip was placed over the isolated gonad and gentle pressure was applied to generate a monolayer of spermatocytes and spermatids. The spreads were immediately analyzed using Nomarski/DIC optics while simultaneously illuminating the specimen with UV epifluoresence to visualize the DNA. For DAPI/tubulin immunostaining, sperm spreads were generated on ColorFrost Plus slides (Fisher Scientific) in buffer without Hoechst. The samples were freeze–cracked in liquid nitrogen before a 12–20-h incubation in −20°C methanol. Tubulin immunostaining was carried out as above.

Additional somatic and germline defects of L1 upshifted animals were analyzed either under DIC optic in living, agar-mounted adult animals (Sulston and Horvitz, 1977), or by UV epifluorescence in whole-mount, DAPI-stained animals that had been fixed in Carnoy II fixative (6:3:1 ethanol/acetic acid/chloroform).

Physical Mapping of emb-27

emb-27 lies within the gene subcluster of LGII (Cassada et al., 1981). Fine-scale genetic mapping studies using a large set of overlapping deficiencies placed *emb-27* to the right of *unc-105* (Sigurdson et al., 1984) and to the left of *mig-5* (Guo, 1995). The cloning and physical mapping of *unc-105* and *mig-5* to the cosmids C41C4 (Liu et al., 1996) and TO5C12 (Guo, 1995), respectively, positioned *emb-27* to a region of three overlapping cosmids, C41C4, F10B5, and TO5C12. Information from the *C. elegans* Sequencing Center was used to identify candidate genes from this region.

RNA-mediated Interference (RNAi)

An expressed sequence tag clone of F10B5.6 (CEESZ14) was used as the template for CeCdc16 cDNA synthesis. CEESZ14 is a truncated cDNA that contains the last 20% of the predicted F10B5.6 open reading frame and the 3′ untranslated region. M13 forward and reverse primers were used to amplify this cDNA insert. Sense and antisense RNAs were synthesized using a T3 and T7 in vitro transcription kit (Ambion). The RNA synthesis reactions were mixed and incubated at 70°C to denature the RNAs and then slow cooled at room temperature to anneal the complementary strands. Young wild-type adult hermaphrodites were microinjected by standard protocols (Mello et al., 1991) with dsRNA, and they were allowed to recover 12 h before analysis by DIC microscopy or fixation for DNA staining. Similar methods were used to analyze the RNAi phenotypes of other *emb-27* gene candidates.

cDNA Synthesis and DNA Sequencing

Total RNA was prepared from wild-type and *emb-27(g48)* hermaphrodites by standard RNA isolation methods. First strand cDNA was prepared with a reverse transcription–PCR kit according to the manufacturer's instructions (Gene Amp Reverse Transcription-PCR; PerkinElmer). F10B5.6-specific cDNAs were PCR amplified with oligonucleotide primers corresponding to either the SL1 trans-spliced leader RNA or the predicted start codon coupled with a primer that contained the predicted translation stop codon. The PCR products were gel purified using Wizard columns (Promega) and cloned into a pBluescript vector (Stratagene). Automated DNA sequencing of the F10B5.6 cDNA was performed using standard methods. A contiguous consensus contig was generated by the CAP Sequence Assembly program (Huang, 1992) accessed via the Baylor College of Medicine Search Launcher. Two independent PCR reactions were sequenced for both wild-type and *g48,* and they were used to determine the consensus sequence of both the wild-type and *g48* F10B5.6 gene sequence.

Results

emb-27(g48) Mothers Produce Meiotic One-Cell Arrested Embryos

Our initial interest in mutants that arrest at the metaphase to anaphase transition of meiosis I arose from our analysis of the maternal effect embryonic lethal (Mel) mutant *emb-27(g48)*. The *emb-27(g48)* mutant was originally isolated in a genetic screen for ts Mel mutants (Cassada et al., 1981). *emb-27(g48)* was reported to produce embryos that arrested at the one-cell stage and failed to form polar bodies, the discarded karyocytes of oocyte meiotic divisions (Denich et al., 1984). Although the terminal phenotype of the mutant *emb-27(g48)* embryos has been reported to be somewhat variable, growth under strict temperature conditions (see Materials and Methods) resulted in a highly penetrant and consistent meiotic one-cell arrest.

Whereas wild-type hermaphrodites contain rapidly cleaving embryos of many different ages, *emb-27*(*g48*) mutant hermaphrodites contain only one-cell embryos (Fig. 1, A and B). Typically, wild-type hermaphrodites have only a single newly fertilized embryo that is at the same meiotic one-cell stage as the entire clutch of *emb-27* embryos. A similar early arrest phenotype has been observed for embryos in which the expression of three *C. elegans cdc-25* genes has been disrupted by RNAi; both *emb-27(g48)* and *cdc-25 (RNAi)* embryos arrest at the one-cell stage without forming pronuclei (Ashcroft, N., and A. Golden, manuscript in preparation). This phenotype is distinct from cleavage-defective mutants such as *air-2* and *cyk-1*,

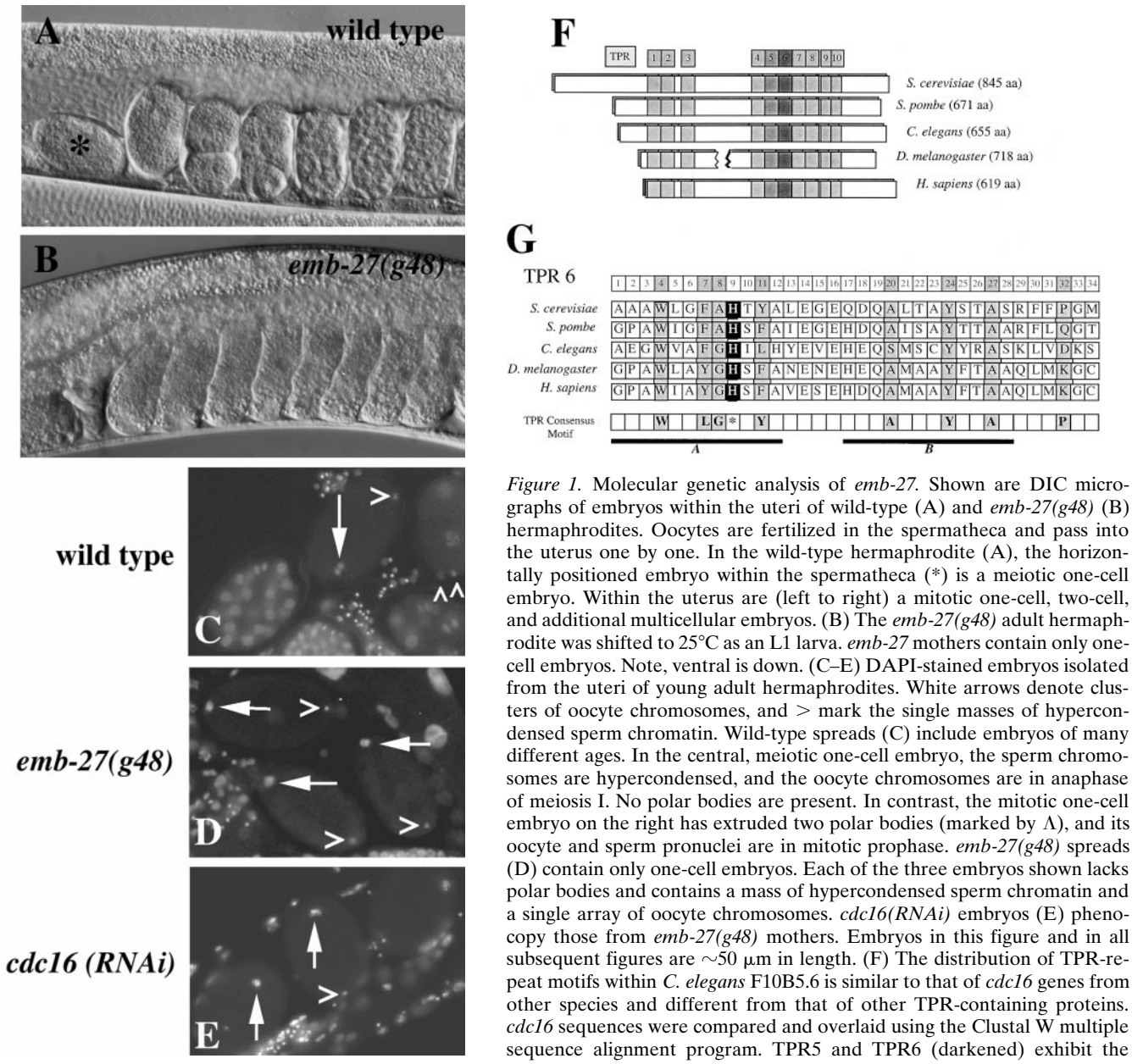

Figure 1. Molecular genetic analysis of *emb-27.* Shown are DIC micrographs of embryos within the uteri of wild-type (A) and *emb-27(g48)* (B) hermaphrodites. Oocytes are fertilized in the spermatheca and pass into the uterus one by one. In the wild-type hermaphrodite (A), the horizontally positioned embryo within the spermatheca (*) is a meiotic one-cell embryo. Within the uterus are (left to right) a mitotic one-cell, two-cell, and additional multicellular embryos. (B) The *emb-27(g48)* adult hermaphrodite was shifted to 25°C as an L1 larva. *emb-27* mothers contain only one-cell embryos. Note, ventral is down. (C–E) DAPI-stained embryos isolated from the uteri of young adult hermaphrodites. White arrows denote clusters of oocyte chromosomes, and > mark the single masses of hypercondensed sperm chromatin. Wild-type spreads (C) include embryos of many different ages. In the central, meiotic one-cell embryo, the sperm chromosomes are hypercondensed, and the oocyte chromosomes are in anaphase of meiosis I. No polar bodies are present. In contrast, the mitotic one-cell embryo on the right has extruded two polar bodies (marked by Λ), and its oocyte and sperm pronuclei are in mitotic prophase. *emb-27(g48)* spreads (D) contain only one-cell embryos. Each of the three embryos shown lacks polar bodies and contains a mass of hypercondensed sperm chromatin and a single array of oocyte chromosomes. *cdc16(RNAi)* embryos (E) phenocopy those from *emb-27(g48)* mothers. Embryos in this figure and in all subsequent figures are ~50 μm in length. (F) The distribution of TPR-repeat motifs within *C. elegans* F10B5.6 is similar to that of *cdc16* genes from other species and different from that of other TPR-containing proteins. *cdc16* sequences were compared and overlaid using the Clustal W multiple sequence alignment program. TPR5 and TPR6 (darkened) exhibit the highest degree of cross-species amino acid sequence identity. An extended region of the *Drosophila melanogaster* sequence has been deleted to emphasize the relative alignment of the TPR motifs. (G) Sequence alignment of TPR6. Each TPR consists of 34 amino acids; the conserved hydrophobic residues are shaded in light gray. These residues lie on the hydrophobic faces of the two amphipathic α helices (residues 1–12 and 17–28; A and B, respectively) (Blatch and Lassle, 1999). The asterisk at position 9 denotes the conserved histidine (shaded in black) that is altered to a tyrosine in *emb-27(g48)*. The sequence data for the wild-type *emb-27* gene is available from GenBank/EMBL/DDBJ under accession no. AF314467.

which arrest at the one-cell stage but nevertheless complete meiosis, exit M phase, and produce pronuclei (Schumacher et al., 1998; Swan et al., 1998).

Before fertilization, *emb-27* oocytes are indistinguishable from their wild-type counterparts. When stained with the DNA dye DAPI, diakinetic *emb-27* oocytes were found to contain a normal complement of six bivalents, indicating that the early meiotic events of homologue pairing, homologous recombination, and chromosome condensation occurred normally. As in wild-type animals, mature *emb-27* oocytes undergo nuclear envelope breakdown just before ovulation. After fertilization, they exhibit many, but not all, of the normal events of egg activation. For instance, the fertilized *emb-27 (g48)* oocytes assume an oval-shaped morphology and initiate eggshell deposition (Fig. 1 B). However, none of these mutant embryos progress beyond the normal meiotic one-cell stage ($n > 200$) (Fig. 1, B and D). DAPI staining of the mutant *g48* embryos revealed that both the sperm chromosomes and oocyte chromosomes remain condensed and positioned near the cortex. This persistent pattern, a cluster of tightly arrayed oocyte chromosomes and a single sperm chromatin mass (Fig. 1 D), is identical to what occurs during the normally transient, meiotic one-cell stage of wild-type embryogenesis (Fig. 1 C). Likewise, the eggshells of *emb-27* embryos remain osmotically sensitive, another

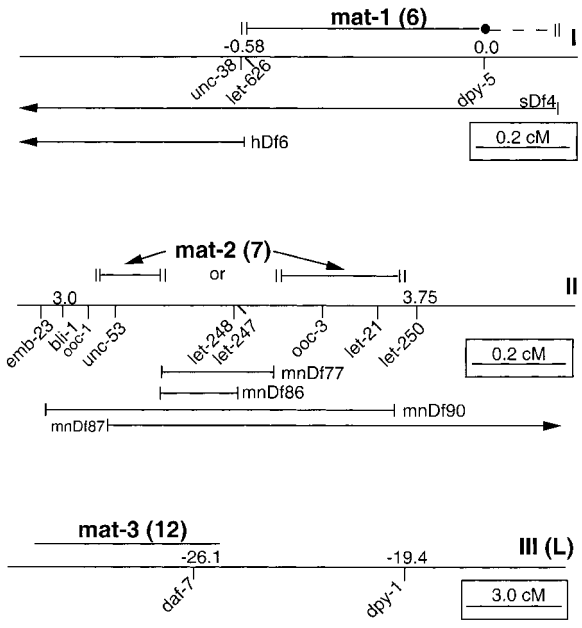

Figure 2. Genetic map of the *mat* mutants and *emb-27* and *emb-30*. See Materials and Methods for genetic details.

characteristic of wild-type meiotic one-cell embryos. These features distinguish *emb-27* embryos from unfertilized oocytes, which remain spherical in shape, fail to form eggshells, and contain a single, centrally located mass of endoreduplicating oocyte chromosomes.

emb-27 Encodes a Subunit of the APC/C

Genetic and physical map data positioned *emb-27* within a three cosmid region on chromosome II (Materials and Methods). Because our attempts to identify *emb-27* by germline transformation rescue proved inconclusive, information from the *C. elegans* Sequencing Center was used to identify *emb-27* candidate genes. Of these genes, only F10B5.6 yielded an *emb-27*–like, one-cell arrest phenotype (Fig. 1 E) by RNAi. This result prompted us to sequence F10B5.6 from the *emb-27(g48)* mutant.

Reverse transcription–PCR was used to amplify the full-length cDNA of F10B5.6 from wild-type and *emb-27 (g48)* animals. Sequencing and translational analysis of the wild-type cDNA confirmed the Genefinder predicted structure of F10B5.6 as a 655 amino acid protein, and analysis of the *g48* cDNA identified a C to T base change at position 1,150 of the cDNA sequence. This change results in a His354Tyr alteration in the amino acid sequence (Fig. 1 G). A BLAST search (Altschul et al., 1990) using the entire F10B5.6 sequence identified the *CDC16* gene from *Saccharomyces cerevisiae* as the closest match (20% identity and 40% similarity over 561 amino acids).

CDC16 is an evolutionarily conserved component of the APC/C (King et al., 1995; Morgan, 1999). Structurally, the Cdc16p subunit contains 10 tetratricopeptide repeats (TPR) (Sikorski et al., 1990), tandem arrays of which form an amphipathic groove that mediates protein–protein interactions (Blatch and Lassle, 1999). TPR proteins are typically described by the number and distribution of their TPR repeats, and F10B5.6 contains the same pattern of TPR repeats as Cdc16p (*S. cerevisiae*) and its *Saccharomyces pombe* ortholog, Cut9p (Fig. 1 F). The *g48* mutation lies within TPR6, the TPR within Cdc16p that exhibits the highest degree of interspecies sequence identity (Samejima and Yanagida, 1994; this study) (Fig. 1 G). The *C. elegans* sequence is 29% identical and 65% similar to the *S. cerevisiae* sequence in this region. The mutated His354 is conserved in all Cdc16 proteins sequenced to date, but it is not one of the conserved hydrophobic residues that defines the TPR motif itself. Instead, this histidine is positioned on the hydrophilic face of α helix A (Das et al., 1998), and, thus, the mutation is predicted to alter both the hydrophobicity and charge of this helical face. Taken together, these data indicate that *emb-27* encodes the *C. elegans* CDC16 ortholog, and that this APC/C subunit is essential for proper APC/C function.

Identification and Isolation of Additional emb-27–like Mutants

Because Cdc16 is only 1 of the 8–12 APC/C subunits, it seemed likely that genetic screens for similar one-cell arrest mutants would identify mutants in additional APC/C and APC/C-related genes. Using the *emb-27(g48)* phenotype as a guide, we screened preexisting collections of ts Mel mutants for additional members of this class. From several different mutant collections (Miwa et al., 1980; Wood et al., 1980; Cassada et al., 1981), we identified two such genes: *emb-1(hc57, hc62)* and *emb-30(g53)* (Fig. 2). Although *emb-1* has not yet been cloned, *emb-30* encodes an ortholog of APC4 (Furuta et al., 2000).

We also initiated a large scale screen for new one-cell arrested ts mutants. Our goal was to isolate additional alleles of *emb-1*, *emb-27*, and *emb-30*, as well as novel members of this phenotypic class. To facilitate the isolation of Mel mutants, screens were carried out in a genetic background of an egg laying–defective mutant (*lin-2*) (Kemphues et al., 1988). The mutant phenotypes were scored in hermaphrodites that had been upshifted to the restrictive temperature of 25°C as L4 larvae. Of ~1.9 million haploid genomes screened, >1,400 ts Mel mutants were isolated. Of these, 44 mutants produced one-cell embryos when homozygous L4s were shifted to 25°C, and 32 of these exhibited meiotic progression defects similar to those of *emb-27(g48)*. Mapping crosses and complementation tests revealed that seven of these mutants are new alleles of *emb-27* (6 alleles) and *emb-30* (1 allele), whereas the remaining 25 alleles define three new complementation groups: *mat-1* (6 alleles), *mat-2* (7 alleles), and *mat-3* (12 alleles). The genetic map positions of these genes are shown in Fig. 2.

Meiotic One-Cell Mutant Embryos Are Blocked in Metaphase of Meiosis I

Between fertilization and the first mitotic division, the one-cell stage of *C. elegans* embryogenesis encompasses the meiotic divisions of the oocyte, a round of DNA synthesis, the conjunction of the pronuclei, and anterior–posterior polarization of the embryo (Albertson, 1984; Albertson and Thomson, 1993; Kemphues and Strome, 1997;

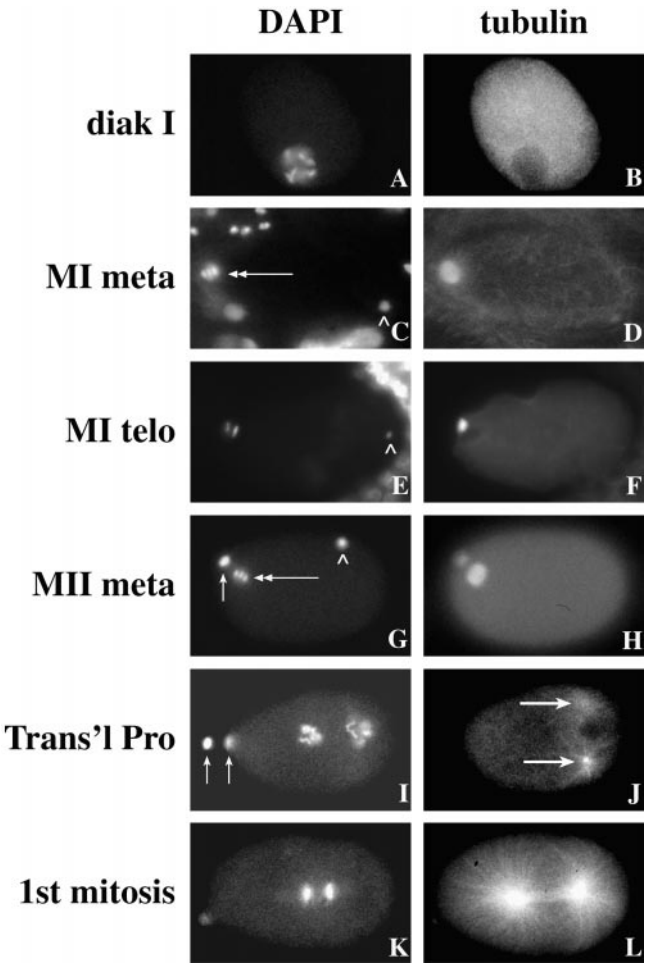

Figure 3. Tubulin and DAPI localization during meiotic progression of wild-type oocytes before and after fertilization. Shown in A, C, E, G, I, and K are DAPI images, and in B, D, F, H, J, and L are the corresponding tubulin images. An oocyte in diakinesis of meiotic prophase I (diak I) is shown in A and B. The subsequent stages after fertilization are depicted: meiosis I metaphase (C and D, MI meta), meiosis I telophase (E and F, MI telo), meiosis II metaphase (G and H, MII meta), transitional prophase (I and J, Trans'l Pro) of the first mitotic cell cycle, and then first mitosis (K and L). During metaphase of meiosis I, the six bivalents are often distinguishable as a "pentagonal array" or, in side view, as a cluster of three axially aligned bivalents (C). During rotation, chromosomes enter anaphase and often up to 12 distinguishable homologues can be visualized at this time. By the time rotation is complete (E and F), the homologues have moved apart towards the opposite spindle poles. Univalents are no longer distinguishable. The oocyte meiotic chromosomes are indicated by double arrows (C and G). Polar bodies, the discarded meiotic products, are indicated by vertical arrows (G and I). In C, E, and G, the condensed sperm chromatin (marked with Λ) marks the future embryonic posterior. The duplicated sperm asters are indicated by arrows (J). *C. elegans* embryos are ~50 μm in length.

Sadler and Shakes, 2000). Fig. 3 shows DNA and tubulin images of the events that lead up to the first mitosis in wild-type embryos. Before fertilization, the primary oocytes undergo a prolonged pause in diakinesis of meiosis I. At this stage, they contain six highly condensed bivalents within a nuclear envelope and a uniform meshwork of cytoplasmic tubulin (Fig. 3, A and B) (Albertson, 1984). Immediately before fertilization, they undergo meiotic maturation, which includes nuclear envelope breakdown (McCarter et al., 1999). After fertilization, the oocyte-derived bivalents align and congress to form a metaphase plate with the five autosomal bivalents surrounding the sex chromosome bivalents in an axial orientation. This arrangement appears as either a "pentagonal array," or, in side view, as a cluster of two or three axially aligned bivalents (Fig. 3 C). The associated meiotic spindle is a barrel-shaped structure that lies adjacent and parallel to the cortex (Fig. 3 D) (Albertson and Thomson, 1993). During this time, the quiescent sperm chromatin remains as a single mass of condensed DNA near its site of entry (Sadler and Shakes, 2000). During anaphase, the spindle rotates to its telophase position, perpendicular to the cortex (Fig. 3, E and F), before extruding one set of oocyte chromosomes into the polar body (Fig. 3 G). Meiosis II proceeds in a similar manner (Fig. 3, G and H) (Albertson, 1984). After these meiotic divisions, the maternal and paternal chromosomes decondense, are encased within nuclear envelopes, and undergo DNA synthesis (Sadler and Shakes, 2000). During this same period, the sperm centrioles duplicate and begin nucleating microtubules (Fig. 3 J) (Albertson, 1984). Subsequently, the zygote enters a period of transitional prophase during which the maternal pronucleus migrates posteriorly to meet the paternal pronucleus (Fig. 3, I and J). The joined pronuclei then move centrally before initiating mitosis (Fig. 3 L).

To further investigate the mutant defects, oocytes and embryos of adult-upshift mutant mothers were examined. No prefertilization defects were detected; DAPI staining revealed the expected six bivalents per oocyte and maturation defects were undetectable by DIC optics. To analyze defects after fertilization, wild-type and mutant embryos were costained with DAPI and anti-tubulin antibodies. Embryos within the uteri of wild-type mothers ranged in age from the 1–50-cell stage (Fig. 4, A and B), and, because the 1-cell stage lasts <1 h at 25°C (Ward and Carrel, 1979; McCarter et al., 1999), only one or two of these embryos were at the one-cell stage of development. In contrast, each of the mutant mothers were filled with 1-cell embryos, all of which were arrested at the same stage of development (Fig. 4, C–N, compare with Fig. 3, C and D). Within the mutant embryos, the oocyte chromosomes had properly congressed and aligned on an acentriolar, barrel-shaped meiotic spindle. However, no evidence of a metaphase to anaphase transition was observed: the homologues remained attached, and the spindle failed to rotate from its initial position parallel to the cortex. On the other side of the embryo, the sperm chromatin mass remained hypercondensed, and the sperm centrosomes remained quiescent. As assessed by DAPI/tubulin staining, all 32 alleles exhibited an identical oocyte meiosis defect; the embryos arrest with what appears to be a normal meiosis I metaphase spindle (compare Fig. 3, C and D, with Fig. 4, C–N). Because these meiotic one-cell mutants share a common metaphase-arrest defect, we call them "*mat*" for metaphase to anaphase transition defective.

mat Mutant Embryos Remain in a Prolonged M phase–like State

Because cell cycle dynamics are ultimately regulated by the activation and inactivation of cyclin-dependent kinases (CDKs) (Gitig and Koff, 2000), the phosphorylation state

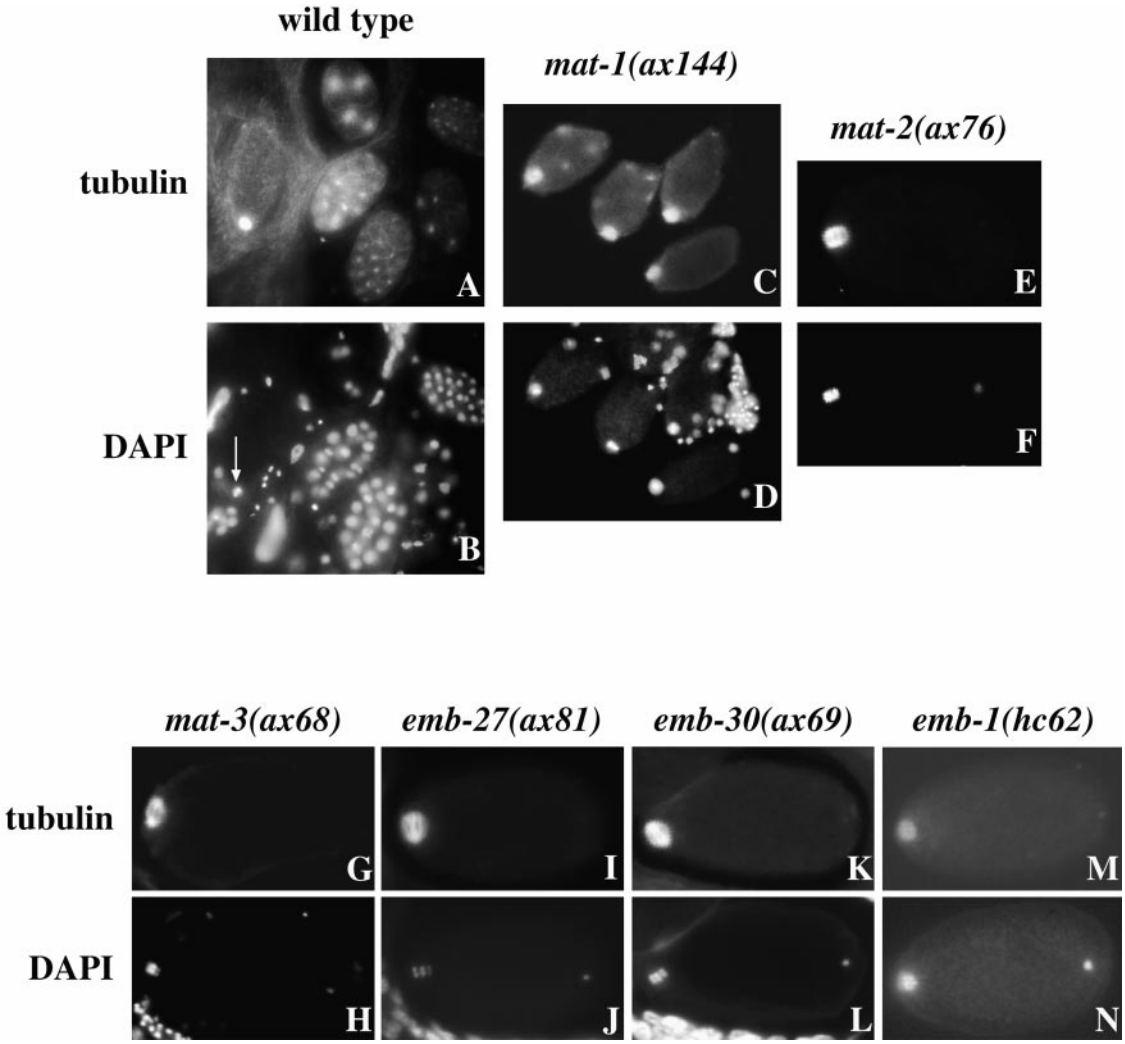

Figure 4. Tubulin and DAPI localization in one-cell arrested *mat* embryos. Wild-type and *mat* mutant adults were shifted to 25.5°C for 6–7 h before embryos were dissected from their mothers. Shown in A and B are a spread of embryos from a wild-type mother. Wild-type animals display a range of developmental stages from meiotic and mitotic one-cells to multicellular. An embryo in metaphase of meiosis I is visible on the left in A; an arrow marks its chromosomes in B. Shown in C and D are a spread of embryos from a *mat-1(ax144)* mother in which all the embryos are arrested in metaphase of meiosis I. E–N show single embryos stained with an anti-tubulin antibody (E, G, I, K, and M). The corresponding DAPI image is shown below each tubulin image. Anterior is to the left. Of these mutants, only *emb-1(hc62)* was not identified in our genetic screens. In most images, the hypercondensed sperm chromatin mass is visible at the right end of each embryo.

of direct and indirect CDK targets can also be used to determine the stage of cell cycle arrest. For instance, histone H3 is phosphorylated during M phase entry and subsequently dephosphorylated before M phase exit (Su et al., 1998; Wei et al., 1998, 1999). Therefore, to test whether the mutant embryos remain in a prolonged M phase state, embryos were analyzed using an antibody against phosphorylated histone H3 (phospho-H3). In both wild-type and mutant embryos, anti–phospho-H3 antibodies intensely stained oocyte chromosomes in their metaphase configuration (Fig. 5). In the mutants, the oocyte chromosomes continued to stain even in the oldest in utero embryos, suggesting that the mutant embryos enter, but never leave, M phase. Note that this antibody does not recognize the highly condensed sperm chromatin mass in either wild-type or mutant embryos (Fig. 5).

Mutant embryos were also analyzed using the MPM-2 monoclonal antibody that recognizes various mitotic phosphoproteins (Davis et al., 1983). The MPM-2 epitope is widely conserved, as this antibody stains kinetochores, centrosomes, and microtubules during early, but not late, M phase (Vandre et al., 1984; Hecht et al., 1987; Vandre and Borisy, 1989; Hirano and Mitchison, 1991; Renzi et al., 1997). As shown in Fig. 6, MPM-2 stains a "halo" of material around or, in some case, between the congressed oocyte meiotic chromosomes in both wild-type (Kitagawa and Rose, 1999) and mutant embryos. MPM-2 also stains the sperm chromatin mass (Fig. 6). In the mutants, MPM-2 continued to stain the chromosomes in older embryos, a further indication that these aging embryos remain blocked in M phase.

Terminal Phenotype

Under stringent conditions, every allele from this ts mutant collection exhibits a block in both the meiosis I metaphase to anaphase transition and in M phase exit. Nevertheless, after 3–4 h at 25.5°C, the oocyte and sperm

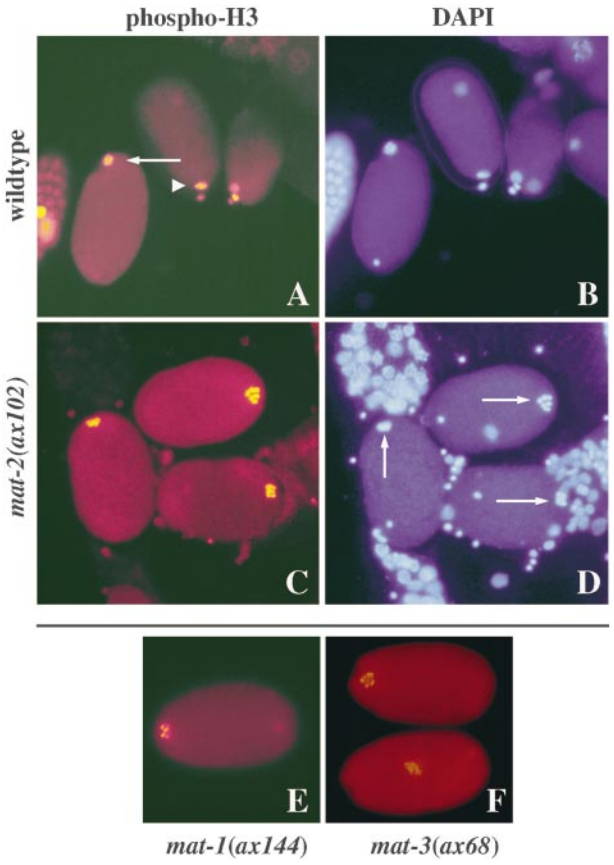

Figure 5. Phosphohistone H3 and DAPI localization in one-cell arrested *mat* embryos. Embryos were dissected from mothers that had been upshifted to 25°C for 6–7 h (A and B). The three wild-type, one-cell stage embryos are in meiosis I metaphase (left), meiosis II metaphase (middle), and S phase (right), based on their DNA staining patterns (B). In the wild-type panels, phosphohistone H3 stains the pentagonal array of the oocyte metaphase meiosis I chromosomes (arrow), but it does not stain the sperm chromatin mass on the other side of the embryo. In the middle embryo, the sperm chromatin mass is out of focus. Phosphohistone H3 brightly stains both the oocyte meiosis II chromosomes (arrowhead) and the chromatin within the adjacent polar body. In the S phase embryo, phosphohistone H3 stains the two polar bodies and the oocyte pronucleus, but not the male pronucleus, which, in this particular embryo, lies next to the oocyte pronucleus. All three *mat-2(ax102)* embryos are in metaphase of meiosis I (D), and their congressed chromosomes (D, arrows) stain brightly (C). Congressed chromosomes also stain in *mat-1(ax144)* (E) and *mat-3(ax68)* (F). (F) The bottom *mat-3* embryo is older and displays the terminal phenotype; the chromosomes continue to stain with phospho-H3 antibody, but have moved centrally and lost their condensed metaphase chromosome morphology. The out of focus DAPI-stained body in the top embryo in D is outside of the embryo.

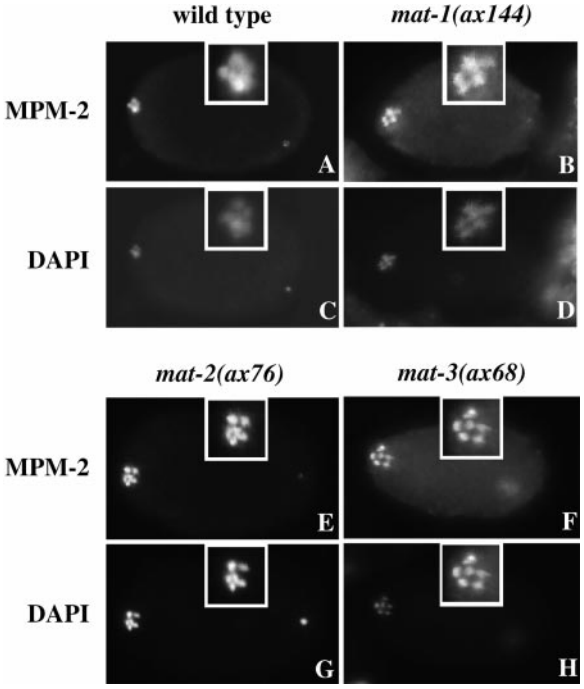

Figure 6. MPM-2 and DAPI localization in one-cell arrested *mat* embryos. Embryos were dissected from mothers that had been shifted to 25°C for 6–7 h. These embryos were stained with the MPM-2 monoclonal antibody (A, B, E, and F) and DAPI (C, D, G, and H) to identify congressed M phase–like chromosomes (A, B, E, and F). Wild-type embryos in metaphase of meiosis I (A and C) are shown compared with arrested *mat-1* (B and D), *mat-2* (E and G), and *mat-3* (F and H) embryos. Note, anterior is to the left. In most images, the hypercondensed sperm chromatin mass is visible at the right end of each embryo. A magnified view of the oocyte chromosomes are shown in each panel.

DNA within the aging mutant embryos leave their position near the cortex and move centrally, and the metaphase chromosomes begin to unravel. Importantly, this DNA unraveling is distinct from DNA decondensation, since the unraveled DNA continues to stain with the phospho-H3 antibody (Fig. 5 F, bottom embryo), and it never become encased within a nuclear envelope (data not shown).

When mutant mothers were grown under suboptimal conditions (e.g., growth at 20–24°C or after brief upshifts), their mutant embryos were sometimes observed to exit M phase and reform nuclear envelopes in the absence of chromosome separation. Other embryos even underwent a few rounds of mitotic cell divisions. The particular conditions required to produce these hypomorphic phenotypes are allele specific, and the hypomorphic defects themselves are consistent with the previously reported phenotypes of both *emb-27(g48)* and *emb-30(g53)* (Cassada et al., 1981), as well as *emb-1*(*hc62* and *hc57)* (Miwa et al., 1980).

Mutant Spermatocytes Are Also Blocked in Metaphase of Meiosis I

In *C. elegans*, the first meiotic division of the oocyte takes place on an acentriolar barrel-shaped meiotic spindle and culminates in a highly unequal division in which one set of homologues are discarded into a tiny polar body. In contrast, the first meiotic division of a primary spermatocyte takes place on a centriole-based, mitotic-like spindle, and, though cytokinesis is often incomplete, the division culminates in the symmetric division of the primary spermatocyte into two secondary spermatocytes (Ward et al., 1981) (Fig. 7 A). Unlike oocytes, in which the first meiotic division only occurs after fertilization, spermatocytes initiate their first meiotic division autonomously as soon as they mature and separate from the syncytial gonad. This first meiotic division is followed by a round of centriole duplication and the assembly of a bipolar meiosis II spindle, orthogonal to the first division axis. The separation of sister chromatids during meiosis II is accompanied by an unusual asymmetric division (spermatid budding) during

Figure 7. Tubulin and DAPI localization in wild-type and mutant spermatocytes. Shown in A is a depiction of wild-type spermatogenesis. After nuclear envelope breakdown, the chromosomes of primary (1°) spermatocytes congress to form a meiosis I metaphase plate. The first meiotic division yields two secondary (2°) spermatocytes, which can either be separated or remain attached through a cytoplasmic connection due to incomplete cytokinesis. Secondary spermatocytes subsequently undergo a polarized budding division during which two haploid sperm separate from a central residual body. (B) A wild-type male germline squashed in the presence of Hoechst dye 33342 and observed by DIC and UV epifluorescence. All meiotic stages can be seen. Primaries (1°) and secondaries (2°) can be distinguished by size (B). A budding figure (BF) is visible in the lower right corner. Haploid sperm (S) and residual bodies (RB) are also indicated. (C) A sperm spread from a *mat-3(ax82)* male lacks 2° spermatocytes, but contains many anucleate sperm. Abnormal budding figures are also present in which all the chromosomes remain in the center of the developing residual body. Staining with anti–α-tubulin antibody (E, G, I, and K) and DAPI (D, F, H, and L) reveals the underlying spindle structures in these sperm spreads (E, G, I, and K). In wild-type sperm spreads, distinctive meiotic spindles are apparent in 1° and 2° spermatocytes and in budding figures (D and E). A magnified view of a wild-type meiotic spindle is shown in (I) with its corresponding DAPI image (H). In the *mat* mutants, normal meiosis I–like spindles form, but anaphase figures are never observed (F, G, J, and K). The diameter of a primary spermatocyte equals 12 μm.

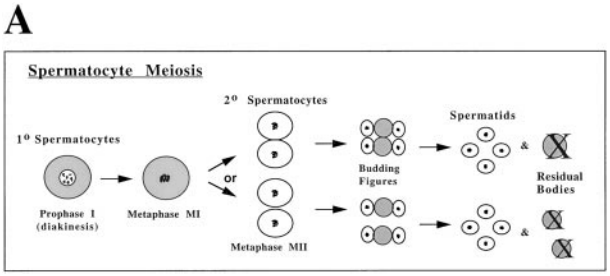

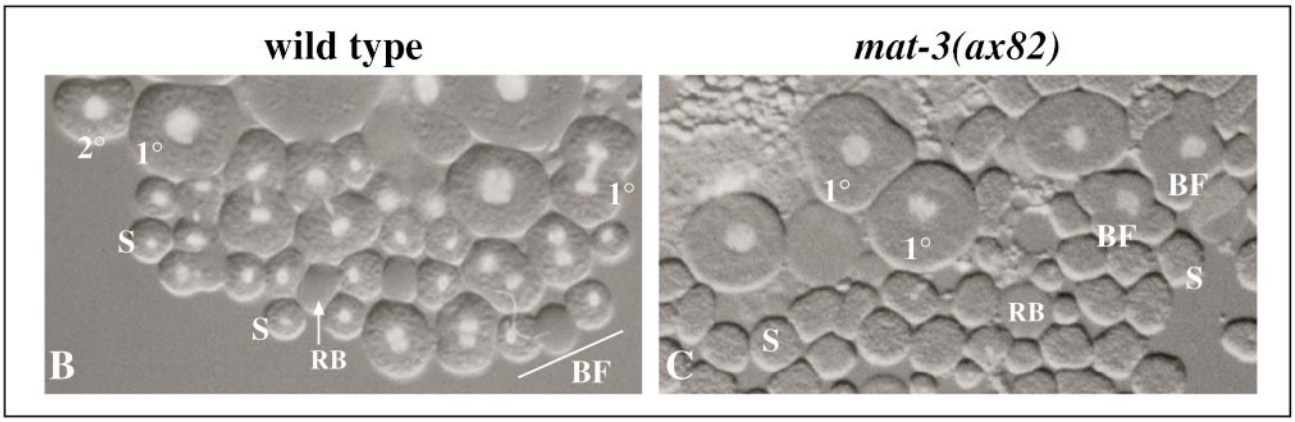

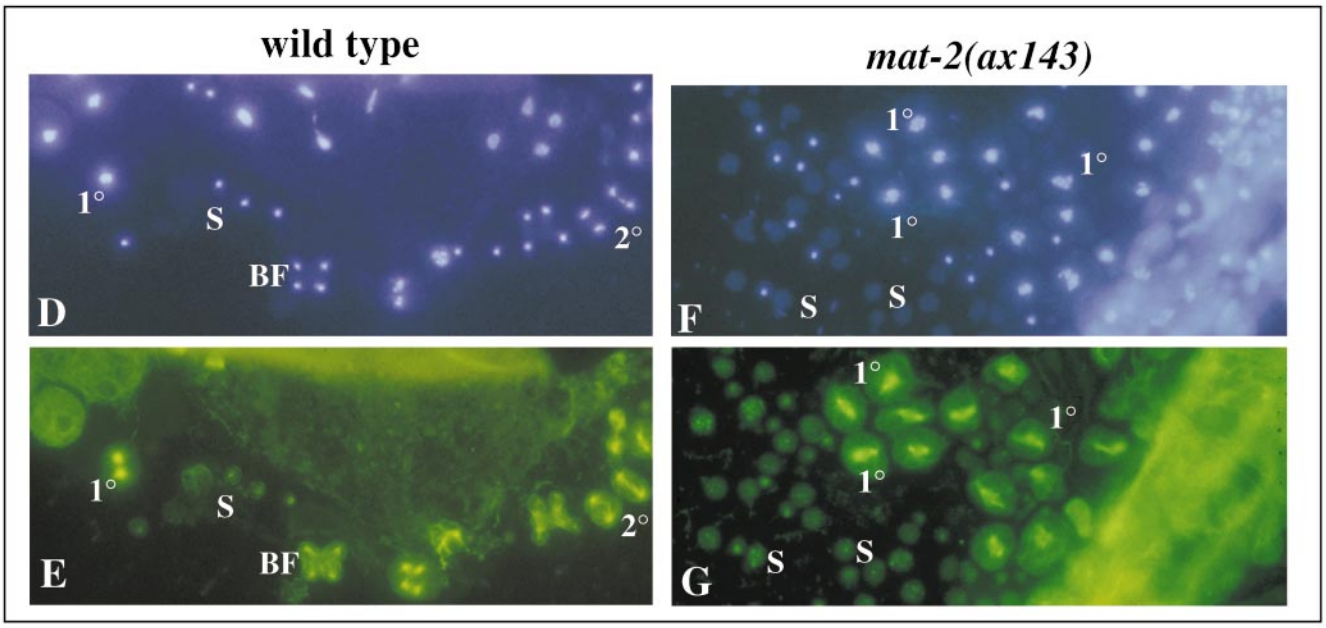

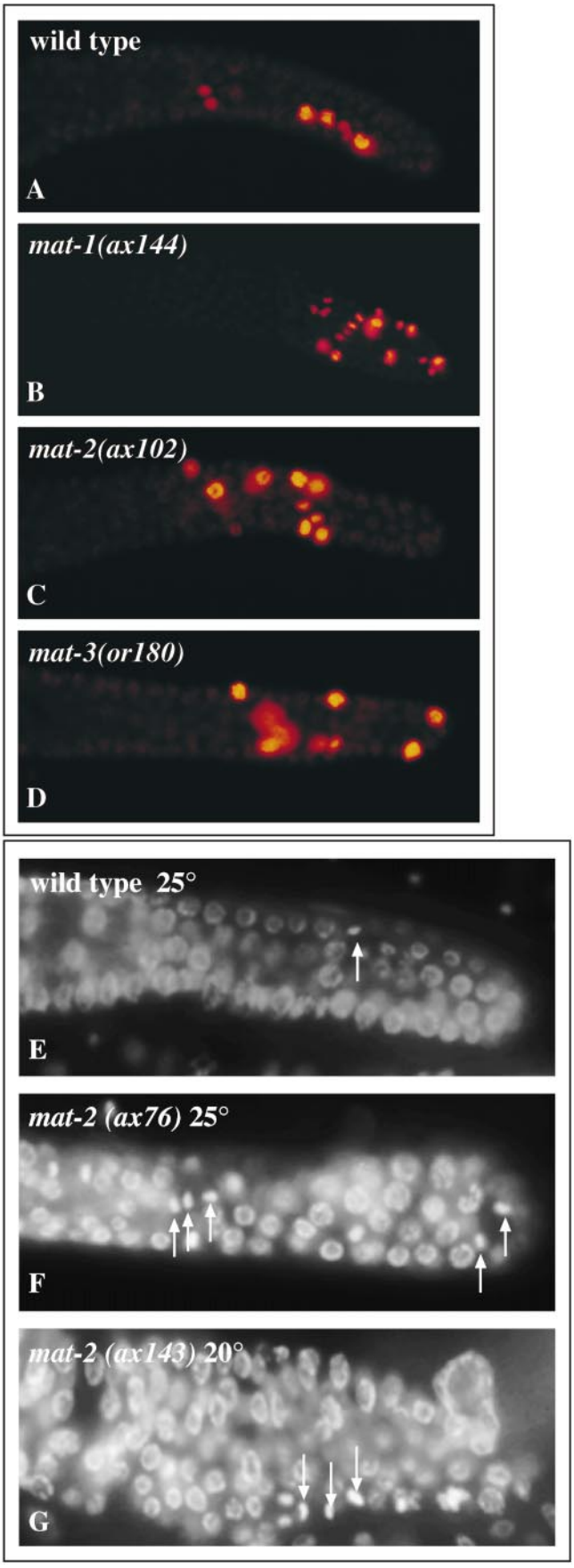

Figure 8. Phospho-H3 staining of adult upshifted wild-type (A), *mat-1(ax144)* (B), *mat-2(ax102)* (C), and *mat-3(or180)* (D) hermaphrodites reveals an excess of mitotic plates in the mitotic region of germlines from isolated mutant gonads. DAPI staining also reveals fewer mitotic figures in the wild-type (E) than *mat-2(ax76)* (F) or *mat-2(ax143)* (G) gonads. Some phenotypes were more obvious at an intermediate temperature of 20°C (G).

which the two haploid sperm bud from a large residual cytoplast (Fig. 7 A).

Given these striking differences between oocyte and spermatocyte meiosis, we investigated whether the *mat* genes functioned in both processes. Testes from young adult mutant males, which had been upshifted to 25.5°C as L3 larvae, were isolated and processed for DIC/Hoechst analysis. Such "sperm spreads" from wild-type males contain cells in all stages of spermatogenesis, including primary spermatocytes, secondary spermatocytes, budding figures, and haploid sperm (Fig. 7 B). In contrast, *mat* mutant spreads exhibit a striking abundance of primary spermatocytes and sperm (Fig. 7 C). Notably, secondary spermatocytes are completely absent, and the DNA staining patterns suggest that meiosis in the mutant primary spermatocytes fails to progress past meiosis I. Despite this apparent meiosis I arrest, cells that resemble haploid sperm still form, but they lack DNA (which we refer to as anucleate). Similar sperm spreads were seen for most *mat* alleles (data not shown) under L3 shift-up conditions, with the striking exceptions that *mat-3 (or172, or180,* and *or187)* and *emb-1 (hc62* and *hc57)* males produce morphologically normal secondary spermatocytes and haploid sperm and can sire viable offspring when mated to feminized hermaphrodites (data not shown) (Sadler, P., D. Fox, A. Pletcher, and D. Shakes, unpublished observations). As previously reported for *emb-27* and *emb-30* males (Sadler and Shakes, 2000), affected *mat-1*, *mat-2*, and *mat-3* males are unable to sire viable offspring, however, their anucleate sperm are surprisingly functional in that they can activate, crawl, and even fertilize oocytes.

To further understand the meiotic defects, we analyzed stage-specific DNA and tubulin structures in wild-type and mutant sperm spreads. In wild-type animals (Fig. 7, D and E), sperm spreads reveal a diversity of microtubule structures ranging from the large, closely opposed asters of the metaphase primary spermatocytes to the highly dynamic spindles of the secondary spermatocytes and budding figures. In *mat* mutants, including *mat-2(ax143)* (Fig. 7, F and G), sperm spreads are dominated by large spermatocytes, each of which contains a metaphase array of chromosomes and a bipolar, astral, meiosis I metaphase spindle. In enlarged views (Fig. 7, H–K), these spindles are closely associated with properly congressed and aligned metaphase chromosomes. Some of the mutant spindles eventually elongate, but homologue separation and other anaphase events never occur. Thus, with the possible exception of *emb-1*, whose two alleles lack spermatocyte defects, these data indicate that every *mat* gene is required for the meiosis I metaphase to anaphase transition in both oocytes and spermatocytes.

The mat Genes Are Also Required for Germline Mitosis

Our analysis of oocyte and spermatocyte meiosis in the mutants suggested that the *mat* gene products function in a

Table I. Quantitation of Phospho-H3–Positive Nuclei in the Distal Germlines of mat Mutants

Gene (allele)	Nuclei	*n*	Significance*
N2 (wild-type)	5.0 ± 2.2	50	
mat-1 (*ax161*)	5.0 ± 3.0	22	NS
mat-1 (*ax144*)	9.8 ± 5.7	32	<0.005
mat-2 (*ax76*)	5.4 ± 2.5	51	NS
mat-2 (*ax102*)	8.3 ± 2.6	38	<0.005
emb-27 (*ax348*)	3.8 ± 2.5	22	NS
emb-27 (*ax162*)	7.1 ± 3.8	35	<0.005
mat-3 (*or180*)	8.6 ± 3.5	55	<0.005
mat-3 (*ax68*)	9.8 ± 4.3	32	<0.005
emb-1 (*hc57*)	7.2 ± 3.8	22	<0.005
emb-1 (*hc62*)	7.1 ± 3.9	24	<0.01

Young adult *mat* hermaphrodites were shifted to 25°C for 6 h and then were dissected to release their gonads. Gonads were fixed and stained with the phospho-H3 antibody. Shown here is quantitation of the number of phospho-H3 positive germ cell nuclei per gonad arm.
*Statistical comparison to N2 using a one tail *t*-test.
n = number of gonadal arms scored.

shared step of these two structurally dissimilar meiotic processes. To address whether these *mat* genes function specifically to separate axially aligned homologues during meiosis I or whether they also function to separate sister chromatids during mitosis, we examined the mitotic divisions of germline nuclei within adults. Because germline mitotic divisions continue at a time when the animal's somatic cells have ceased to divide (Beanan and Strome, 1992), they can be studied in adult upshifted mutants in the absence of potential complications from somatic defects. To test for mitotic defects, young adult hermaphrodites were upshifted to 25°C for 6 h. When isolated wild-type gonads were immunostained with phosphohistone H3 antibodies, they were found to contain one to six mitotic germ cell nuclei in the distal region of each gonadal arm (Fig. 8, A–D, Table I). In an allele-specific manner, mutant gonads had either slightly or greatly elevated numbers of phospho-H3 staining mitotic germ cell nuclei (Fig. 8; Table I). DAPI staining of these mitotic nuclei revealed that most of the phospho-H3–positive nuclei are in metaphase (Fig. 8, E–G), though anaphase figures are also common, particularly in weaker alleles. We believe that the excess in mitotic figures stems from an extended block or pause in metaphase, rather than an increased cell cycle rate, since upshifts of longer duration result in reduced rather than tumorous germlines (data not shown).

Although these initial studies indicated a role for *mat* genes in the "maintenance" of the mitotic germline pool in adults, they did not address whether the *mat* genes are also required for the initial proliferation of the germline. Newly hatched *C. elegans* larvae contain only two germline progenitor cells, Z2 and Z3, that must proliferate during larval development to generate the >1,000 germ cell nuclei of the mature adult gonad (Kimble and White, 1981). To test whether *mat* genes are required for the initial expansion of the germline, mutants were upshifted as newly hatched L1 larvae. For some alleles, the earlier upshift conditions did not significantly alter the mutant phenotype; these Mel adults had fully proliferated germlines and produced large broods of one-cell arrested embryos (Table II). For other alleles, these same conditions caused moderate to severe defects in germline proliferation (Table II and data not shown). In the most severe cases, L1 upshifts resulted in sterile (Ste) adults with fewer than 50 germ cells and no apparent gametes. Similar defects in mitotic germline proliferation have been reported for null alleles of *emb-30* (Furuta et al., 2000).

In Embryos and Larvae, the mat Genes Are Also Essential for Somatic Cell Divisions

To investigate whether the *mat* genes are also required for mitotic cell divisions of the soma, mutant hermaphrodites and males were upshifted as L1 larvae and examined for potential somatic defects. Although our analysis did not include all 32 alleles, we observed that a subset of alleles within the *mat-1*, *mat-2*, *mat-3*, and *emb-27* complementation groups exhibit defects in somatic development. For instance, for *mat-1(ax144)* animals, >40% of the hermaphrodites have protruding vulvae, and >90% of males have tails with missing or abnormal ray structures (data not shown). Similar somatic defects were reported for a subset of *emb-30* alleles (Furuta et al., 2000). For three *mat-3* alleles, the animals are also uncoordinated, suggesting defects in the proliferation of cells that make up the ventral nerve cord. The hermaphrodite vulva, male tail, and ventral nerve cord are all structures that require substantial numbers of larval cell divisions, and the spectrum of observed phenotypes resemble those of cell cycle mutants in which postembryonic divisions have been disrupted (O'Connell et al., 1998; Boxem et al., 1999; Park and Krause, 1999; Woollard and Hodgkin, 1999). We have not yet determined whether these somatic defects are caused by arrest or delays in the mitotic cell cycle.

In an attempt to generate stronger somatic defects, two-cell embryos, which had completed both oocyte meiosis and the first mitotic division at 16°C, were dissected from their mothers and directly upshifted to 25°C. Our complete set of ts alleles were tested in this manner, and, in most cases, these two-cell embryos underwent normal embryogenesis and developed into adults. Depending on the allele, the adults either produced broods of one-cell embryos (Mel) or were Ste (Table II). In most cases, the phenotype of the two-cell and the L1 larval upshifts did not differ; in others, embryonic upshifts enhanced the germline proliferation, hermaphrodite vulva, male tail, and/or uncoordinated defects described above (data not shown). The unexpected mildness of the observed somatic defects, particularly in upshifted two-cell embryos, may suggest that these *mat* genes function in only a subset of mitotic divisions. Alternatively, our results may be explained by maternal rescue, gene redundancy, or the fact that these ts alleles are unlikely to be genetic nulls.

Discussion

In summary, we have isolated and characterized a large set of ts mutant alleles that define five complementation groups and share a common defect: mutant mothers shifted to the nonpermissive temperature of 25°C produce embryos that arrest at the meiotic one-cell stage. Our premise, that these affected one-cell embryos reach a normal meiosis I metaphase state, but then fail to progress to anaphase, is supported by the following observations: (a) the oocytes undergo normal maturation events and, after fertilization, their chromosomes align and congress in a

Table II. Phenotypes of mat Mutants after Shift-Ups at Different Stages

	Allele	L4 shift-up	L1 shift-up	Two-cell shift-up
mat-1 (LG I):	*ax161, ax227*	Mel	Mel	Mel
	ax144, ax212	Mel	Ste	Ste
mat-2 (LG II):	*ax76, ax78, or170*	Mel	Mel	Mel
	ax102, ax142, ax143, or224	Mel	Ste	Ste
mat-3 (LG III):	*ax148, or172, or180, or187*	Mel	Mel	Mel
	ax68, ax70, ax71, ax77, ax79	Mel	Ste	Ste
	ax82, ax136, or192	Mel	Ste	Ste
emb-27:	*ax348, g48*	Mel	Mel	Mel
	ax80, ax81, ax162, or279	Mel	Ste	Ste
emb-30:	*ax69, g53*	Mel	Mel	Mel
emb1:	*hc57, hc62*	Mel	Mel	Mel
Nonconditional alleles: *mat-1(ax72), mat-1(ax520), emb-27 (ax189)*				

Shown here are the 32 alleles recovered in the screen for the Mat phenotype. Also included are the previously existing alleles of *emb-27 (g48)*, *emb-30 (g53)*, and *emb-1* (*hc57* and *hc62*) that belong in this class of Mat mutants. All *ax* and *or* alleles were identified based on L4 shift-up experiments in which L4s produce entire broods of one-cell arrested embryos at 25°C (and hence are Mel). Shift-up experiments were also carried out with L1 larvae. Most L1 larvae shifted to 25°C developed to the adult stage and produced broods of one-cell embryos (Mel) or were Ste. Shift-up experiments with two-cell embryos were also carried out: most hatched and developed to the adult stage where they were either Mel or Ste. The phenotypes shown for the two-cell shift-ups represents the phenotypes of those embryos that hatched. For some alleles, a fraction of the embryos routinely die before hatching, regardless of the temperature conditions. In this table, the Ste category is broad, ranging from hermaphrodites with little or no germline to hermaphrodites that produce one or two embryos. The three alleles listed at the bottom were isolated in the ts screen, but proved to be nonconditional upon outcrossing.

metaphase pentagonal array on a morphologically normal meiotic spindle, (b) in such embryos, the sperm chromatin remains condensed and the sperm microtubule organizing center remains quiescent, and (c) neither meiotic anaphase figures nor polar bodies are ever observed. In addition, the stable presence of phosphohistone H3 and MPM-2 epitopes indicates that the mutant embryos are permanently arrested in an M phase–like state. These results suggest that functional meiotic CDKs drive the mutant embryos into metaphase of meiosis I, but because these CDKs are not subsequently deactivated, the mutant embryos are unable to transition out of a metaphase state. Thus, we have chosen the name "*mat*" (defined above) as an appropriate designation for this general mutant class.

Importantly, the metaphase to anaphase transition defects in these mutants are not restricted to oocyte meiosis I. Analogous defects are observed during spermatogenesis: primary spermatocytes undergo normal budding from the gonadal syncytium, undergo nuclear envelope breakdown, but then arrest in a normal meiosis I metaphase state and never form secondary spermatocytes. Thus, the same fundamental defect is seen in both spermatocyte and oocyte meiosis, despite the fact that spermatocytes employ astral, rather than anastral spindles. On the other hand, the developmental consequences of this common meiosis I block are strikingly dissimilar. The mutant oocytes appear to be blocked from further development as their sperm chromatin remains condensed and their sperm-contributed microtubule organizing centers remain quiescent. In contrast, differentiation of the mutant spermatocytes proceeds with the eventual formation of motile, albeit anucleate, spermatozoa.

These mutants also display metaphase to anaphase transition defects during mitosis. Most dramatically affected are the mitotic divisions of proliferating germ cells; upshifted adults accumulate an excessive number of phospho-H3–staining germ cell nuclei, and upshifted larvae exhibit moderate to severe defects in germ cell proliferation. However, unlike the complete metaphase blocks observed during meiosis, the metaphase block during germ cell mitosis is frequently incomplete and results in an M phase delay. The identification of defects in somatic tissues, such as the male tail and the hermaphrodite vulva, suggests that the *mat* genes are also required for mitotic divisions of the soma.

Each of the *mat* genes, except for *emb-1*, is represented by an allelic series that encompasses the full range of described metaphase to anaphase transition defects. Because identical mutant defects are observed in multiple alleles of multiple genes, they are likely to reflect important functions of this gene class. Thus, our data implies that a common mechanism governs the transition from metaphase to anaphase, regardless of whether this transition (a) involves the separation of homologues or sister chromatids, (b) is mediated by anastral or astral spindles, (c) occurs within syncytial or nonsyncytial cells, or (d) involves germline or somatic cells. On the other hand, whereas all of the mutant alleles have defects in oocyte meiosis and most have defects in spermatocyte meiosis, many fewer exhibit defects in the mitotic divisions of either the germline or soma. Furthermore, we observed strong metaphase blocks during meiosis I, but primarily M phase delays during germline mitosis. Thus, whereas the *mat* genes are required for all of these various cell divisions, meiotic divisions may be particularly sensitive to low levels of gene product. Alternatively, the design of our mutant screens may have favored the isolation of mutants with lesions in meiotic-specific or germline-specific domains. Sequence analysis of the mutant lesions may preferentially support one of these two explanations, and, in the latter case, identify specific functional subdomains within each protein.

What is the molecular nature of these genes that are required for the metaphase to anaphase transition during various types of cell divisions? Evidence from the cell cycle literature suggests that mitotic metaphase blocks can stem either from defects in the machinery that drives the metaphase to anaphase transition or from spindle and/or kinetochore attachment defects that secondarily trigger the metaphase checkpoint system. Recent studies suggest that this checkpoint is functioning within one-cell *C. elegans* embryos (Kitagawa and Rose, 1999), but, because the *mat* mutants assemble morphologically normal metaphase plates and spindles, we suspect the *mat* genes encode com-

ponents of the cell cycle machinery per se. Consistent with this hypothesis, we report that *emb-27* encodes an ortholog of the APC/C subunit, Cdc16. Molecular analysis of the other *mat* genes is ongoing, but we have recently discovered that *mat-1* encodes an ortholog of another APC/C gene, *cdc27* (Schumacher, J., D. Shakes, and A. Golden, manuscript in preparation), and Furuta et al. (2000) report that *emb-30* encodes APC4. Thus, the Mat phenotype appears to be an excellent predictor of APC/C and APC/C-related genes, and it is not surprising that *emb-1*, *mat-2*, and *mat-3* all map to regions in which APC/C subunits have been identified.

It is somewhat surprising that this large mutant screen, which is at or near saturation, yielded multiple alleles of only five genes (*emb-1* was not reisolated), all of which are either known or likely to encode conserved APC/C components. First, this screen was expected to identify several meiosis-specific APC "accessory proteins" or regulators that enable the APC/C to separate homologues during meiosis I without disrupting the centromeric sister chromatid cohesions that are APC/C's primary, but indirect target, during mitosis and meiosis II. Although our results do not rule out the existence of such modifiers, they do indicate that such modifiers do not easily mutate to temperature sensitivity. This result suggests that APC/C functions largely in the same capacity in distinct types of cell divisions. Second, even if all six *mat* genes prove to encode APC/C subunits, there are at least nine APC/C subunits encoded within the *C. elegans* genome (King et al., 1995, Yu et al., 1998; Zachariae et al., 1998; Furuta et al., 2000; Wille, L., and D. Shakes, manuscript in preparation). It is not clear why additional genes were not hit, but similar ts screens in yeast likewise identified only a subset of APC/C genes. Thus, something about either the function or molecular structure of the individual subunits must make them more or less likely to be isolated in such ts screens. This possibility is supported by studies in *S. cerevisiae* in which only a small number of essential genes could be mutated to be ts (Kaback et al., 1984; Harris and Pringle, 1991).

The phenotypic analysis of this large set of ts *mat* mutants and the molecular identification of *emb-27* as an ortholog of Cdc16 have enabled us to define an essential role for APC/C in a variety of specialized cell divisions, including the first meiotic division of both oocytes and spermatocytes. Importantly, our analysis reveals that all of these metaphase to anaphase transitions are driven by a common cellular mechanism, and that many or all of the individual APC/C subunits are essential for M phase progression in these various cell types. Ts mutants proved critical to our analysis, since meiotic functions could not have been analyzed in nonconditional mutants with defects in germline proliferation. In continuing studies, analysis of the molecular lesions associated with each allele should reveal which protein domains are important for general and/or cell-type–specific functions. Additionally, screens for genetic suppressers may identify additional components that act in each of these pathways.

Many thanks to Michael Krause, Ann Corsi, Orna Cohen-Fix, and members of the Bowerman, Golden, Seydoux, and Shakes laboratories for helpful discussions and comments on the manuscript. We also gratefully acknowledge Neville Ashcroft, Mary Kosinski, Ilsa Kaattari for their excellent technical support, A.R. Kerlavage (The Institute for Genomic Research) for providing the CEESZ14 cDNA, and the *C. elegans* Genetics Center (University of Minnesota), funded by the NIH National Center for Research Resources, for providing mapping strains.

This work was supported in part by grants from the National Science Foundation (IBN92653092 to D. Shakes), the National Institutes of Health (IR15GM60359-01 to D. Shakes, 1RO1GM58017-02 to B. Bowerman), the American Cancer Society (to G. Seydoux, PF-4444 to D. Hamill), the Jeffress Memorial Trust (J387 to D. Shakes), the Packard Foundation (to G. Seydoux), the March of Dimes (to G. Seydoux), and Howard Hughes Medical Institute (Undergraduate Biological Sciences Education grant to the College of William and Mary).

Submitted: 28 August 2000
Revised: 27 October 2000
Accepted: 1 November 2000

References

Albertson, D.G. 1984. Formation of the first cleavage spindle in nematode embryos. *Dev. Biol.* 101:61–72.

Albertson, D.G., and J.N. Thomson. 1993. Segregation of holocentric chromosomes at meiosis in the nematode, *Caenorhabditis elegans*. *Chromosome Res*. 1:15–26.

Altschul, S.F., W. Gish, W. Miller, E.W. Myers, and D.J. Lipman. 1990. Basic local alignment search tool. *J. Mol. Biol.* 215:403–410.

Beanan, M.J., and S. Strome. 1992. Characterization of a germ-line proliferation mutation in *C. elegans*. *Development*. 116:755–766.

Blatch, G.L., and M. Lassle. 1999. The tetratricopeptide repeat: a structural motif mediating protein-protein interactions. *Bioessays*. 21:932–939.

Blose, S.H., D.I. Meltzer, and J.R. Feramisco. 1984. 10-nm filaments are induced to collapse in living cells microinjected with monoclonal and polyclonal antibodies against tubulin. *J. Cell Biol*. 98:847–858.

Boxem, M., D.G. Srinivasan, and S. van den Heuvel. 1999. The *Caenorhabditis elegans* gene ncc-1 encodes a cdc2-related kinase required for M phase in meiotic and mitotic cell divisions, but not for S phase. *Development*. 126: 2227–2239.

Brenner, S. 1974. The genetics of *Caenorhabditis elegans*. *Genetics*. 77:71–94.

Cassada, R., E. Isnenghi, M. Culotti, and G. von Ehrenstein. 1981. Genetic analysis of temperature-sensitive embryogenesis mutants in *Caenorhabditis elegans*. *Dev. Biol*. 84:193–205.

Ciosk, R., W. Zachariae, C. Michaelis, A. Shevchenko, M. Mann, and K. Nasmyth. 1998. An ESP1/PDS1 complex regulates loss of sister chromatid cohesion at the metaphase to anaphase transition in yeast. *Cell*. 93:1067–1076.

Das, A.K., P.W. Cohen, and D. Barford. 1998. The structure of the tetratricopeptide repeats of protein phosphatase 5: implications for TPR-mediated protein-protein interactions. *EMBO (Eur. Mol. Biol. Organ.) J*. 17:1192–1199.

Davis, F.M., T.Y. Tsao, S.K. Fowler, and P.N. Rao. 1983. Monoclonal antibodies to mitotic cells. *Proc. Natl. Acad. Sci. USA*. 80:2926–2930.

Denich, K.T.R., E. Schierenberg, E. Isnenghi, and R. Cassada. 1984. Cell-lineage and developmental defects of temperature-sensitive embryonic arrest mutants of the nematode *Caenorhabditis elegans*. *Wilhelm Roux's Arch. Dev. Biol.* 193:164–179.

Edgar, L.G. 1995. Blastomere culture and analysis. *Methods Cell Biol*. 48:303–321.

Eigsti, O.J., and Dustin P. 1957. Colchicine in Agriculture, Medicine, Biology, and Chemistry. Iowa State College Press, Ames, IA. 470 pp.

Emmons, S.W., M.R. Klass, and D. Hirsh. 1979. Analysis of the constancy of DNA sequences during development and evolution of the nematode *Caenorhabditis elegans. Proc. Natl. Acad. Sci. USA*. 76:1333–1337.

Encalada, S.E., P.R. Martin, J.B. Phillips, R. Lyczak, D.R. Hamill, K.A. Swan, and B. Bowerman. 2000. DNA replication defects delay cell division and disrupt cell polarity in early *Caenorhabditis elegans* embryos. *Dev. Biol.* In press.

Furuta, T., S. Tuck, J. Kirchner, B. Koch, R. Auty, R. Kitagawa, A.M. Rose, and D. Greenstein. 2000. EMB-30: an APC4 homologue required for metaphase-to-anaphase transitions during meiosis and mitosis in *Caenorhabditis elegans*. *Mol. Biol. Cell*. 11:1401–1419.

Gardner, R.D., and D.J. Burke. 2000. The spindle checkpoint: two transitions, two pathways. *Trends Cell Biol*. 10:154–158.

Gitig, D.M., and A. Koff. 2000. Cdk pathway: cyclin-dependent kinases and cyclin-dependent kinase inhibitors. *Methods Mol. Biol*. 142:109–123.

Guo, C. 1995. Mig-5, a gene that controls cell fate determination and cell migration in *C. elegans*. Ph.D. thesis. The Johns Hopkins University, Baltimore, MD.

Harris, S.D., and J.R. Pringle. 1991. Genetic analysis of *Saccharomyces cerevisiae* chormosome I: on the role of mutagen specificity in delimiting the set of genes identifiable using temperature-sensitive-lethal mutations. *Genetics*. 127:279–285.

Hecht, R.M., M. Berg-Zabelshansky, P.N. Rao, and F.M. Davis. 1987. Conditional absence of mitosis-specific antigens in a temperature-sensitive embry-

onic-arrest mutant of *Caenorhabditis elegans*. *J. Cell Sci.* 87:305–314.
Hendzel, M.J., Y. Wei, M.A. Mancini, A. Van Hooser, T. Ranalli, B.R. Brinkley, D.P. Bazett-Jones, and C.D. Allis. 1997. Mitosis-specific phosphorylation of histone H3 initiates primarily within pericentromeric heterochromatin during G2 and spreads in an ordered fashion coincident with mitotic chromosome condensation. *Chromosoma*. 106:348–360.
Hirano, T., and T.J. Mitchison. 1991. Cell cycle control of higher-order chromatin assembly around naked DNA in vitro. *J. Cell Biol*. 115:1479–1489.
Hirsh, D., D. Oppenheim, and M. Klass. 1976. Development of the reproductive system of *Caenorhabditis elegans*. *Dev. Biol*. 49:200–219.
Huang, X. 1992. A contig assembly program based on sensitive detection of fragment overlaps. *Genomics*. 14:18–25.
Juang, Y.L., J. Huang, J.M. Peters, M.E. McLaughlin, C.Y. Tai, and D. Pellman. 1997. APC-mediated proteolysis of Ase1 and the morphogenesis of the mitotic spindle. *Science*. 275:1311–1314.
Kaback, D.B., P.W. Oeller, H.Y. de Steensma, J. Hirschman, D. Ruezinsky, K.G. Coleman, and J.R. Pringle. 1984. Temperature-sensitive lethal mutations on yeast chromosome I appear to define only a small number of genes. *Genetics.* 108:67–90.
Kemphues, K.J., and S. Strome. 1997. Fertilization and embryonic polarity. *In C. elegans* II. D.L. Riddle, T. Blumenthal, B. Meyer, and J.R. Priess, editors. Cold Spring Harbor Laboratory Press, Cold Spring Harbor, NY. 335–359.
Kemphues, K.J., J.R. Priess, D.G. Morton, and N.S. Cheng. 1988. Identification of genes required for cytoplasmic localization in early *C. elegans* embryos. *Cell*. 52:311–320.
Kimble, J.E., and J.G. White. 1981. On the control of germ cell development in *Caenorhabditis elegans*. *Dev. Biol*. 81:208–219.
King, R.W., J.M. Peters, S. Tugendreich, M. Rolfe, P. Hieter, and M.W. Kirschner. 1995. A 20S complex containing CDC27 and CDC16 catalyzes the mitosis-specific conjugation of ubiquitin to cyclin B. *Cell*. 81:279–288.
Kitagawa, R., and A.M. Rose. 1999. Components of the spindle-assembly checkpoint are essential in *Caenorhabditis elegans*. *Nat. Cell Biol*. 1:514–521.
Liu, J., B. Schrank, and R.H. Waterston. 1996. Interaction between a putative mechanosensory membrane channel and a collagen. *Science.* 273:361–364.
McCarter, J., B. Bartlett, T. Dang, and T. Schedl. 1999. On the control of oocyte meiotic maturation and ovulation in *Caenorhabditis elegans*. *Dev. Biol*. 205:111–128.
Mello, C.C., J.M. Kramer, D. Stinchcomb, and V. Ambros. 1991. Efficient gene transfer in *C. elegans*: extrachromosomal maintenance and integration of transforming sequences. *EMBO (Eur. Mol. Biol. Organ.) J*. 10:3959–3970.
Miller, D.M., and D.C. Shakes. 1995. Immunofluorescence microscopy. *Methods Cell Biol*. 48:365–394.
Miwa, J., E. Schierenberg, S. Miwa, and G. von Ehrenstein. 1980. Genetics and mode of expression of temperature-sensitive mutations arresting embryonic development in *Caenorhabditis elegans*. *Dev. Biol*. 76:160–174.
Miyazaki W.Y., and T.L. Orr-Weaver. 1994. Sister-chromatid cohesion in mitosis and meiosis. *Annu. Rev. Genet.* 28: 167–187.
Morgan, D.O. 1999. Regulation of the APC and the exit from mitosis. *Nat. Cell Biol.* 1:E47–E53.
Murray, A., and T. Hunt. 1993. The Cell Cycle: An Introduction. W.H. Freeman and Company, New York. 252 pp.
Nasmyth, K., J.M. Peters, and F. Uhlmann. 2000. Splitting the chromosome: cutting the ties that bind sister chromatids. *Science*. 288:1379–1385.
O'Connell, K.F., C.M. Leys, and J.G. White. 1998. A genetic screen for temperature-sensitive cell-division mutants of *Caenorhabditis elegans*. *Genetics*. 149:1303–1321.
Park, M., and M.W. Krause. 1999. Regulation of postembryonic G(1) cell cycle progression in *Caenorhabditis elegans* by a cyclin D/CDK-like complex. *Development*. 126:4849–4860.
Peters, J.M. 1999. Subunits and substrates of the anaphase-promoting complex. *Exp. Cell Res*. 248:339–349.
Renzi, L., M.S. Gersch, M.S. Campbell, L. Wu, S.A. Osmani, and G.J. Gorbsky. 1997. MPM-2 antibody-reactive phosphorylations can be created in detergent-extracted cells by kinetochore-bound and soluble kinases. *J. Cell Sci*. 110:2013–2025.
Sadler, P.L., and D.C. Shakes. 2000. Anucleate *Caenorhabditis elegans* sperm can crawl, fertilize oocytes and direct anterior-posterior polarization of the one-cell embryo. *Development*. 127:355–366.
Salah, S.M., and K. Nasmyth. 2000. Destruction of the securin Pds1p occurs at the onset of anaphase during both meiotic divisions in yeast. *Chromosoma.* 109:27–34.
Samejima, I., and M. Yanagida. 1994. Bypassing anaphase by fission yeast cut9 mutation: requirement of cut-9+ to initiate anaphase. *J. Cell Biol*. 127: 1655–1670.
Schumacher, J.M., A. Golden, and P.J. Donovan. 1998. AIR-2: an Aurora/Ipl1-related protein kinase associated with chromosomes and midbody microtubules is required for polar body extrusion and cytokinesis in *Caenorhabditis elegans* embryos. *J. Cell Biol*. 143:1635–1646.
Shonn, M.A., R. McCarroll, and A.W. Murray. 2000. Requirement of the spindle checkpoint for proper chromosome segregation in budding yeast meiosis. *Science*. 289:300–303.
Sigurdson, D.C., G.J. Spanier, and R.K. Herman. 1984. *Caenorhabditis elegans* deficiency mapping. *Genetics*. 108:331–345.
Sikorski, R.S., M.S. Boguski, M. Goebl, and P. Hieter. 1990. A repeating amino acid motif in CDC23 defines a family of proteins and a new relationship among genes required for mitosis and RNA synthesis. *Cell*. 60:307–317.
Su, T.T., F. Sprenger, P.J. DiGregorio, S.D. Campbell, and P.H. O'Farrell. 1998. Exit from mitosis in *Drosophila* syncytial embryos requires proteolysis and cyclin degradation, and is associated with localized dephosphorylation. *Genes Dev*. 12:1495–1503.
Sulston, J.E., and H.R. Horvitz. 1977. Post-embryonic cell lineages of the nematode, *Caenorhabditis elegans*. *Dev. Biol*. 56:110–156.
Swan, K.A., A.F. Severson, J.C. Carter, P.R. Martin, H. Schnabel, R. Schnabel, and B. Bowerman. 1998. *cyk-1*: a *C. elegans* FH gene required for a late step in embryonic cytokinesis. *J. Cell Sci*. 111:2017–2027.
Vandre, D.D., and G.G. Borisy. 1989. Anaphase onset and dephosphorylation of mitotic phosphoproteins occur concomitantly. *J. Cell Sci*. 94:245–258.
Vandre, D.D., F.M. Davis, P.N. Rao, and G.G. Borisy. 1984. Phosphoproteins are components of mitotic microtubule organizing centers. *Proc. Natl. Acad. Sci. USA*. 81:4439–4443.
van Heemst, D., and C. Heyting. 2000. Sister chromatid cohesion and recombination in meiosis. *Chromosoma.* 109:10–26.
Ward, S., and J.S. Carrel. 1979. Fertilization and sperm competition in the nematode *Caenorhabditis elegans. Dev. Biol*. 73:304–321.
Ward, S., Y. Argon, and G.A. Nelson. 1981. Sperm morphogenesis in wild-type and fertilization-defective mutants of *Caenorhabditis elegans*. *J. Cell Biol.* 91:26–44.
Wei, Y., C.A. Mizzen, R.G. Cook, M.A. Gorovsky, and C.D. Allis. 1998. Phosphorylation of histone H3 at serine 10 is correlated with chromosome condensation during mitosis and meiosis in *Tetrahymena*. *Proc. Natl. Acad. Sci. USA*. 95:7480–7484.
Wei, Y., L. Yu, J. Bowen, M.A. Gorovsky, and C.D. Allis. 1999. Phosphorylation of histone H3 is required for proper chromosome condensation and segregation. *Cell*. 97:99–109.
Wood, W.B., R. Hecht, S. Carr, R. Vanderslice, N. Wolf, and D. Hirsh. 1980. Parental effects and phenotypic characterization of mutations that affect early development in *Caenorhabditis elegans*. *Dev. Biol*. 74:446–469.
Woollard, A., and J. Hodgkin. 1999. Stu-7/air-2 is a *C. elegans* aurora homologue essential for chromosome segregation during embryonic and post-embryonic development. *Mech. Dev*. 82:95–108.
Yamamoto, A., V. Guacci, and D. Koshland. 1996. Pds1p, an inhibitor of anaphase in budding yeast, plays a critical role in the APC and checkpoint pathway(s). *J. Cell Biol*. 133:99–110.
Yu, J., J.M. Peters, R.W. King, A.M. Page, P. Hieter, and M.W. Kirschner. 1998. Identification of a cullin homology region in a subunit of the anaphase-promoting complex. *Science.* 279:1219–1222.
Zachariae, W., and K. Nasmyth. 1999. Whose end is destruction: cell division and the anaphase-promoting complex. *Genes Dev*. 13:2039–2058.
Zachariae, W., A. Shevchenko, P.C. Andrews, R. Ciosk, M. Galova, M.J. Stark, M. Mann, and K. Nasmyth. 1998. Mass spectrometric analysis of the anaphase-promoting complex from yeast: identification of a subunit related to cullins. *Science*. 279:1216–1219.